

Recent Changes in the Ventilation of the Southern Oceans

Darryn W. Waugh,^{1*} Francois Primeau,² Tim DeVries,³ Mark Holzer⁴

Surface westerly winds in the Southern Hemisphere have intensified over the past few decades, primarily in response to the formation of the Antarctic ozone hole, and there is intense debate on the impact of this on the ocean's circulation and uptake and redistribution of atmospheric gases. We used measurements of chlorofluorocarbon-12 (CFC-12) made in the southern oceans in the early 1990s and mid- to late 2000s to examine changes in ocean ventilation. Our analysis of the CFC-12 data reveals a decrease in the age of subtropical subantarctic mode waters and an increase in the age of circumpolar deep waters, suggesting that the formation of the Antarctic ozone hole has caused large-scale coherent changes in the ventilation of the southern oceans.

The transport of surface waters into the interior ("ventilation") of the southern oceans plays an important role in global climate and the cycling of carbon, oxygen, and nutrients in the oceans (1–3). Over the past few decades, the southern oceans have warmed at roughly twice the rate of the global mean ocean (1), and around 40% of the anthropogenic carbon in the oceans entered south of 40°S (4). Southern ocean

ventilation is driven primarily by the westerly winds (5), which have strengthened and shifted poleward over recent decades, primarily as a consequence of Antarctic stratospheric ozone depletion (6). Modeling studies suggest that this has caused changes in the ocean's overturning circulation (7–9), and carbon uptake (10, 11). However, the sensitivity of the southern ocean circulation and ventilation to decadal changes in wind stresses is under debate (12–14).

Information on ventilation rates can be obtained from measurements of chlorofluorocarbons (CFCs). These compounds are conserved within the oceans, and their atmospheric concentrations have increased rapidly from when they were first produced in the 1930s until the mid-1990s (fig. S1). Because of this time dependence, CFC measurements can provide constraints on the rates and pathways of ocean transport (15, 16).

We used CFC-12 measurements made along several sections in the southern oceans in the early 1990s as part of the World Ocean Circulation Experiment (WOCE) and resampled in mid- to late 2000s as part of the Climate Variability and Predictability (CLIVAR) and CO₂ repeat hydrography program (supplementary materials) to examine changes in the ventilation of the southern oceans over the past two decades.

The measurements during WOCE show largest *p*CFC-12 at the surface, with values decreasing with depth along isopycnals (e.g., Fig. 1A). [We express the measurements as the partial pressure of CFC-12 (*p*CFC-12), defined as the seawater concentration divided by the solubility (16). This enables direct comparison with the atmospheric history of CFC-12.] The repeat occupations 14 to 16 years later show large increases in *p*CFC-12 in the subtropical thermocline (~25° to 45°S, 200 to 1000 m), which correspond to the waters formed by the transport of surface waters along surfaces of constant density (e.g., Fig. 1B). In contrast, very small changes in *p*CFC-12 are observed in polar waters (~50° to 60°S, 200 to 1000 m), where deep water upwells. Figure 1 shows *p*CFC-12 changes for a section in the South Pacific (P16, see Fig. 2A), but similar changes in *p*CFC-12 are observed for other South Pacific sections and for sections in the southern Indian and Atlantic Oceans (16).

Increases in oceanic CFC-12 from the early 1990s to the late 2000s are expected as a consequence of the increasing atmospheric CFC-12 concentrations. To determine whether these changes in CFC-12 imply a temporal change in transport, it is necessary to take into account the nonlinear

¹Department of Earth and Planetary Sciences, Johns Hopkins University, Baltimore, MD 21218, USA. ²Department of Earth System Science, University of California, Irvine, CA 92697, USA. ³Department of Atmospheric and Oceanic Sciences, University of California, Los Angeles, CA 90095, USA. ⁴School of Mathematics and Statistics, University of New South Wales, Sydney, Australia and Department of Applied Physics and Applied Mathematics, Columbia University, New York, NY 10027, USA.

*To whom correspondence should be addressed. E-mail: waugh@jhu.edu

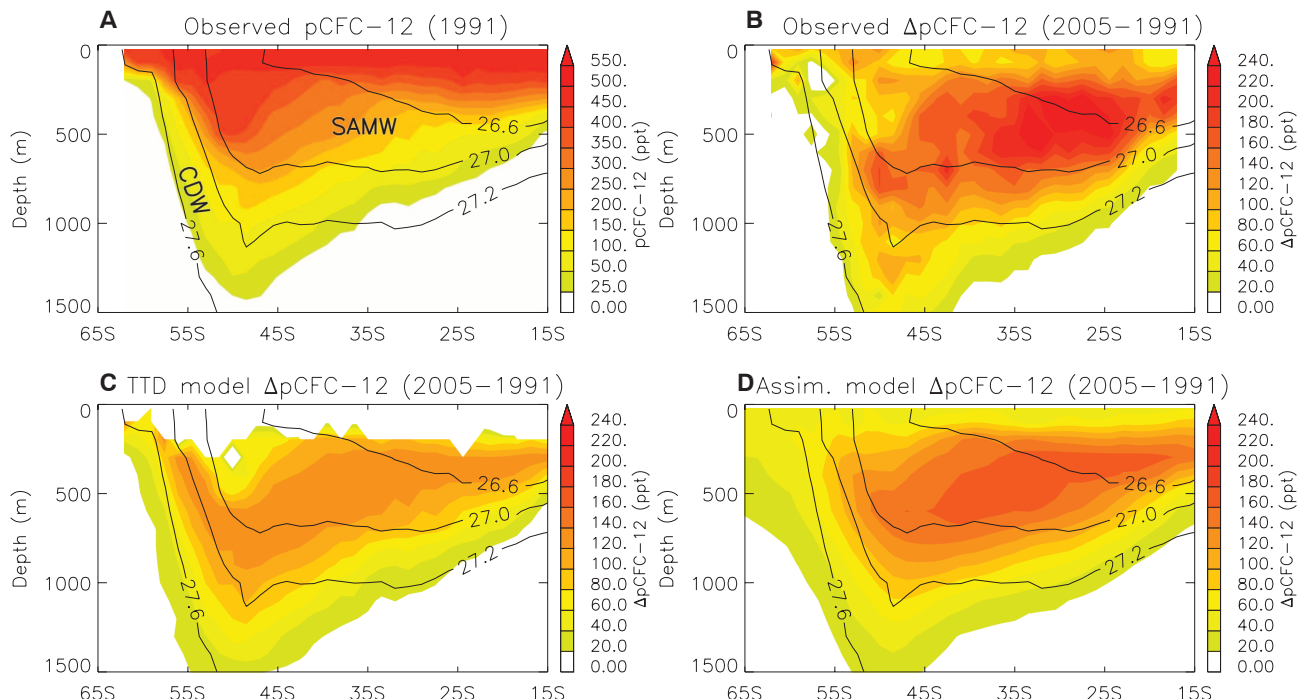


Fig. 1. Depth-latitude cross sections for WOCE P16 section (~150°W; see Fig. 2A): (A) observed *p*CFC-12 in 1991. Changes in *p*CFC-12 between 1991 and 2005 for (B) observations, (C) TTD model, and (D) assimilated model. Contours show potential density referenced to the sea surface σ_0 (kg/m^3). ppt, parts per thousand.

atmospheric growth rate of CFC-12 and the mixing of different water masses. Converting the CFC-12 concentrations into a tracer age (time lag between surface and interior p CFC-12) does not circumvent this need because temporal changes in p CFC ages can occur even for steady transport (17). To examine whether the changes in CFC-12 are consistent with steady transport, we used two very different transport models that include mixing and are constrained to match the observed CFCs in the 1990s. The first has its basis in transit-time distribution (TTD) theory (17, 18), and the second is a data-constrained (“assimilated”) ocean circulation model (19) (supplementary materials).

The null hypothesis to be tested is that the observed changes in CFC-12 between cruises can be explained by steady transport. We therefore used both the TTD model and the assimilated model to make predictions of CFC-12 for the repeat cruise, assuming steady transport between the time of the original cruise and the repeat cruise. Significant differences between modeled and observed CFC-12 at the time of the repeat cruise

then indicate a change in transport rates between the early 1990s and the late 2000s.

The general pattern of the predicted CFC-12 in the South Pacific is similar in both models, with both predicting CFC-12 that tends to be smaller than observed in the subtropical thermocline but larger than observed in the polar waters (Figs. 1, C and D, and 2C). The smaller-than-observed increases in subtropical waters (with largest differences around 25° to 35°S) and larger-than-observed increases in polar waters [with largest differences below the Subantarctic Front (SAF)] also occur for predictions for other South Pacific sections and sections in the southern Indian and Atlantic Oceans (Fig. 2 and fig. S3). There is some small-scale variability in the magnitude, and even sign, of the differences between observed and modeled CFC-12 increases that could be due to mesoscale or interannual variability. To remove the influence of such variability, we examined the CFC-12 increases averaged over entire water masses. Specifically, we calculated the average for subtropical Subantarctic Mode Water (SAMW) (defined as σ_0 between 26.6 and

27.0 kg/m^3) and polar Circumpolar Deep Water (CDW) (potential density anomalies σ_0 between 27.2 and 27.6 kg/m^3) (see supplementary materials for details). These water-mass averages reveal unambiguous large-scale differences between model-predicted and observed CFC-12 increases, with the models predicting larger-than-observed increases in subtropical SAMW and smaller-than-observed increases in polar CDW (Fig. 3A). Furthermore, consistency among the sections, which were first sampled on different dates between 1989 and 1995 and resampled between 2005 and 2010, indicates a coherent decadal-scale change between the early 1990s to late 2000s rather than changes resulting from year-to-year variability.

This conclusion is robust to the method of analysis and to the uncertainties in the models. Despite substantial differences between the two models used (including the form of the TTDs, how the surface concentrations are set, and the data used to constrain the models), both models produce smaller-than-observed increases in SAMW and larger-than-observed increases in polar CDW

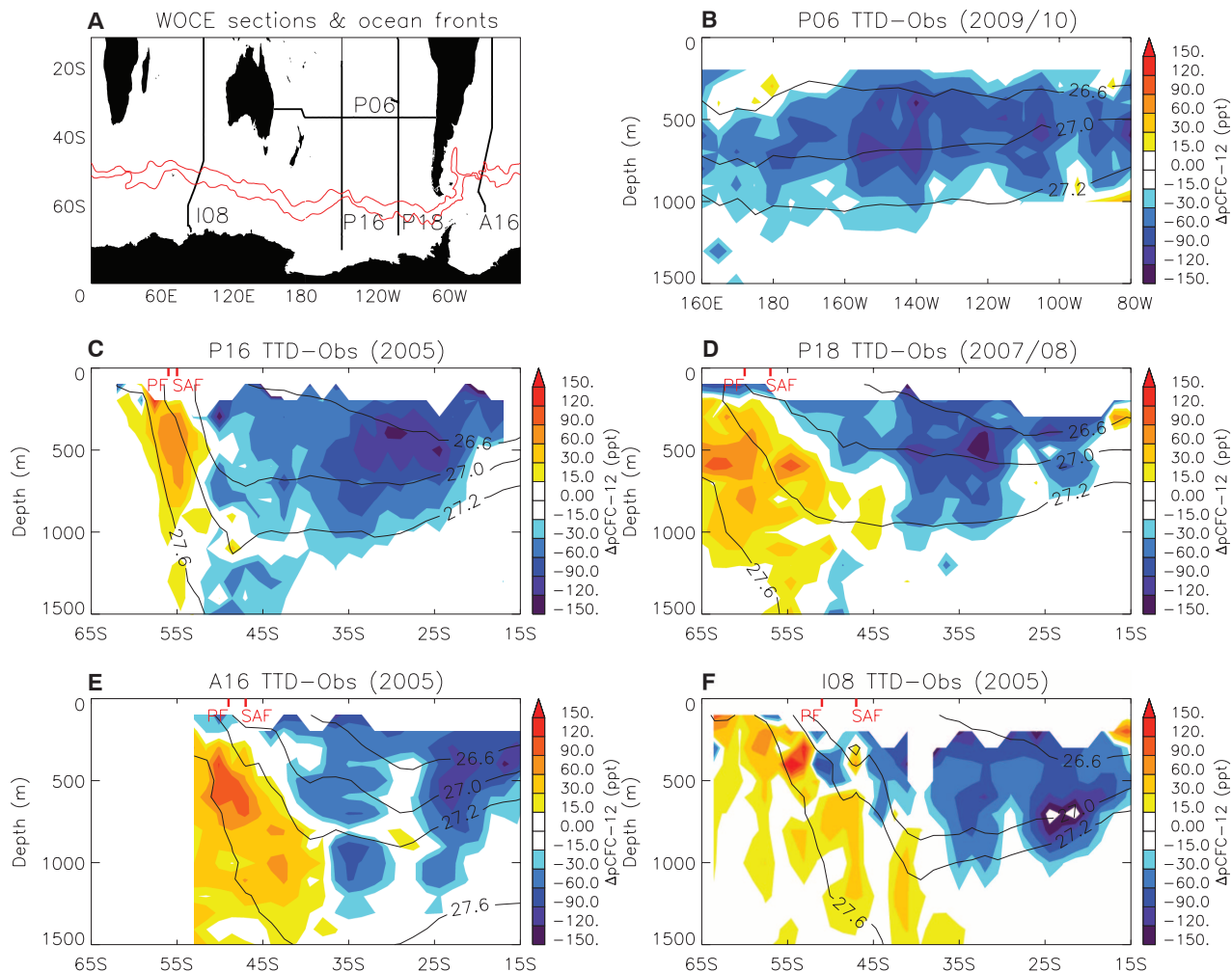


Fig. 2. (A) Map showing sections analyzed, and the climatological polar front (PF) and SAF from (29) (red curves). (B) Depth-longitude and (C to F) depth-latitude cross sections of the difference between TTD-predicted and observed in p CFC-12 for repeat cruise (shading) and isopycnals for first

sampling (contours) of the (B) P06, (C) P16, (D) P18, (E) A16, and (F) I08 sections. The TTD calculations use $\Delta/\Gamma = 1.0$ and surface saturation of 90%. Only the upper 1500 m of each section is shown. The latitudes of the PF and SAF are marked on (C) to (F).

(Fig. 3). Furthermore, differences between the model-predicted CFC-12 and observations are outside the uncertainty associated with the models (Fig. 3A). For the TTD model, this uncertainty includes uncertainty in the ratio of the width to mean age (ΔT) and in the surface saturation of CFC-12. For the assimilation model, the uncertainty is estimated by the difference between modeled and observed CFC-12 measurements for cruises in the 1990s (supplementary materials).

Observed CFC-12 greater than that predicted assuming steady transport from the early 1990s to late 2000s indicates a decrease in the time since water was last at the surface (i.e., younger ages), with the more recent ventilation bringing higher CFC concentrations into the interior ocean. The reverse (older ages) is true if the observed CFC-12 is less than predicted. Thus, the above differences in CFC-12 suggest that there has been a decrease in the age of subtropical SAMW but an increase in the age of polar CDW. We used the TTD method to estimate the change in mean water age Γ between the time of the original CFC-12 measurement (early 1990s) and the repeat measurements (mid- to late 2000s) (supplementary materials). Álvarez *et al.* (20) performed a similar analysis to examine changes in the ventilation of the subtropical eastern Indian Ocean. This is only a rough estimate of the true change in Γ , because it is assumed that changes in the age are captured by the difference in two steady models, each fit to the CFCs independently. Our estimates show that coherent, large-scale age changes occur in the southern Pacific, Indian, and Atlantic Oceans, with 10 to 40% decreases in the age of subtropical SAMW and 30 to 60% increases in the age of polar CDW (Fig. 3B).

The age changes in Fig. 3B are consistent with the expected response of the Southern Ocean circulation to the observed intensification of surface westerly winds (7, 8): Intensified winds lead to

a strengthened and poleward-shifted Ekman divergence and enhanced polar upwelling and to increased northward Ekman transport and formation rates of subtropical mode waters. The spatial patterns of the age changes are further consistent with model-simulated changes in westerly wind strength and water age resulting from anthropogenic climate forcing on centennial time scales (21, 22).

The inferred age changes are also consistent with other ocean observations. They map qualitatively onto the schematic of the observed temperature and salinity changes across a meridional section of the Southern Ocean, with warmer, saltier, and older waters south of the polar front and cooler, fresher, and younger waters north of the polar front (5, 23). Further, they are consistent with the observed intensification of the southern subtropical gyres (24), increases in dissolved oxygen in the subtropical Indian Ocean and decreases in dissolved oxygen in the polar Southern Ocean (25, 26), and a slowdown of carbon uptake in Antarctic waters in recent decades (2) because of enhanced upwelling of polar CDW, which brings old carbon-rich deep waters to the surface.

The ventilation changes inferred here could be due to a number of causes: natural decadal variability, ozone depletion, increased greenhouse gases, or a combination of these. However, the consistency of the inferred age changes with the observed intensification of surface westerly winds, which have occurred primarily because of Antarctic stratospheric ozone depletion (6), suggests that Antarctic ozone depletion is the primary cause.

Future changes in this ventilation will likely depend on the recovery of stratospheric ozone and the magnitude of greenhouse-gas increases. Because the ventilation of SAMW and CDW occurs on decadal and longer time scales, a lag between peak ozone forcing and maximum changes in ocean ventilation is expected (9). As stratospheric

ozone recovers over the next 40 to 60 years, the recent trend of intensifying summer westerly winds may slow or reverse (6, 27, 28). However, continued increases in greenhouse gases will likely lead to strengthened westerlies during other seasons. The integrated impact of these trends in Southern Hemisphere westerlies on the ocean's ventilation and uptake of heat and anthropogenic carbon is an open question.

References and Notes

1. S. T. Gille, *J. Clim.* **21**, 4749 (2008).
2. C. Le Quéré *et al.*, *Science* **316**, 1735 (2007); 10.1126/science.1136188.
3. J. L. Sarmiento, N. Gruber, M. A. Brzezinski, J. P. Dunne, *Nature* **427**, 56 (2004).
4. S. Khattiwala, F. Primeau, T. Hall, *Nature* **462**, 346 (2009).
5. J. R. Toggweiler, J. Russell, *Nature* **451**, 286 (2008).
6. D. W. J. Thompson *et al.*, *Nat. Geosci.* **4**, 741 (2011).
7. A. Hall, M. Visbeck, *J. Clim.* **15**, 3043 (2002).
8. A. Sen Gupta, M. H. England, *J. Clim.* **19**, 4457 (2006).
9. M. Sigmond, M. C. Reader, J. C. Fyfe, N. P. Gillett, *Geophys. Res. Lett.* **38**, L12601 (2011).
10. A. Lenton, R. Matear, *Global Biogeochem. Cycles* **21**, GB2016 (2007).
11. N. S. Lovenduski, N. Gruber, *Geophys. Res. Lett.* **32**, L11603 (2005).
12. C. W. Böning, A. Disper, M. Visbeck, S. R. Rintoul, F. U. Schwarzkopf, *Nat. Geosci.* **1**, 864 (2008).
13. T. Ito, M. Woloszyn, M. Mazloff, *Nature* **463**, 80 (2010).
14. M. P. Meredith, A. C. Naveira Garbato, A. M. Hogg, R. Farneti, *J. Clim.* **25**, 99 (2012).
15. P. Schlosser *et al.*, in *Ocean Circulation and Climate: Observing and Modelling the Global Ocean*, G. Siedler, J. Church, J. Gould, Eds. (Academic Press, New York, 2001).
16. R. A. Fine, *Annu. Rev. Mar. Sci.* **3**, 173 (2011).
17. D. W. Waugh, T. M. Hall, T. W. N. Haine, *J. Geophys. Res.* **108**, 3138 (2003).
18. D. W. Waugh, T. M. Hall, B. I. McNeil, R. Key, *Tellus* **58B**, 376 (2006).
19. T. DeVries, F. Primeau, *J. Phys. Oceanogr.* **41**, 2381 (2011).
20. M. Álvarez *et al.*, *J. Geophys. Res.* **116**, C09016 (2011).
21. F. O. Bryan, G. Danabasoglu, P. R. Gent, K. Lindsay, *Ocean Model.* **15**, 141 (2006).
22. A. Gnanadesikan, J. L. Russell, F. Zeng, *Ocean Sci* **3**, 43 (2007).
23. S. Aoki, N. L. Bindoff, J. A. Church, *Geophys. Res. Lett.* **32**, L07607 (2005).
24. D. Roemmich *et al.*, *J. Phys. Oceanogr.* **37**, 162 (2007).
25. R. J. Matear, A. C. Hirst, B. I. McNeil, *Geochim. Geophys. Geosyst.* **1**, 21 (2000).
26. E. L. McDonagh *et al.*, *J. Clim.* **18**, 1575 (2005).
27. S.-W. Son *et al.*, *Science* **320**, 1486 (2008).
28. C. McLandress *et al.*, *J. Clim.* **24**, 1850 (2011).
29. A. Orsi, U. Harris, Locations of the various fronts in the Southern Ocean, Australian Antarctic Data Centre, Catalogue of Australian Antarctic and Subantarctic Metadata (2001, updated 2008); http://gcmd.nasa.gov/KeywordSearch/Metadata.do?Portal=amd_au&MetadataView=Full&MetadataType=0&KeywordPath=&OrigMetadataNode=AADC&EntryId=southern_ocean_fronts.

Acknowledgments: We thank A. Gnanadesikan, T. Haine, and E. Y. Kwon for helpful conversations and J. Bullister, M. Warner, R. Fine, and the other scientists who provided the CFC-12 data for the WOCE and CLIVAR programs. D.W.W. acknowledges support from NSF grant ANT-1043307, F.P. acknowledges support from NSF grant OCE-0928395, and M.H. acknowledges support from NSF grant ATM-0854711 and Australian Research Council grant DP120100674.

Supplementary Materials

www.sciencemag.org/cgi/content/full/339/6119/568/DC1
Materials and Methods
Figs. S1 to S3
References (30, 31)

30 May 2012; accepted 27 November 2012
10.1126/science.1225411

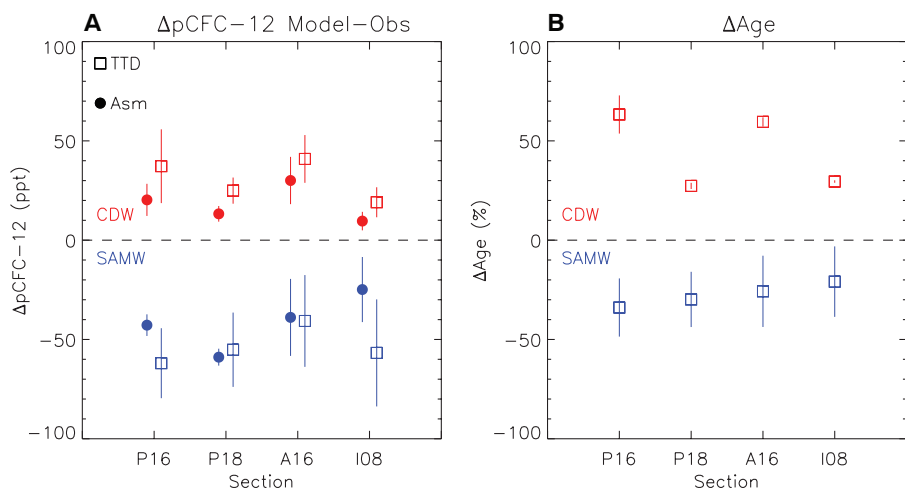


Fig. 3. (A) Difference in simulated and observed increases in $pCFC-12$ for polar CDW (red symbols) and subtropical SAMW (blue) for each meridional section. (B) Percentage difference in mean age for water masses and sections shown in (A). See supplementary materials for description of water mass calculations. The solid circles show values for the assimilation model, whereas the squares show the TTD model. Vertical bars for assimilation model are uncertainties for water-mass averages in the 1990s, whereas for the TTD model they show the standard deviation of TTD calculations obtained by varying $\Delta T/\Gamma$ and surface saturation.

This copy is for your personal, non-commercial use only.

If you wish to distribute this article to others, you can order high-quality copies for your colleagues, clients, or customers by [clicking here](#).

Permission to republish or repurpose articles or portions of articles can be obtained by following the guidelines [here](#).

The following resources related to this article are available online at www.sciencemag.org (this information is current as of September 9, 2015):

Updated information and services, including high-resolution figures, can be found in the online version of this article at:

<http://www.sciencemag.org/content/339/6119/568.full.html>

Supporting Online Material can be found at:

<http://www.sciencemag.org/content/suppl/2013/01/30/339.6119.568.DC1.html>

A list of selected additional articles on the Science Web sites **related to this article** can be found at:

<http://www.sciencemag.org/content/339/6119/568.full.html#related>

This article **cites 28 articles**, 2 of which can be accessed free:

<http://www.sciencemag.org/content/339/6119/568.full.html#ref-list-1>

This article has been **cited by** 2 articles hosted by HighWire Press; see:

<http://www.sciencemag.org/content/339/6119/568.full.html#related-urls>

This article appears in the following **subject collections**:

Oceanography

<http://www.sciencemag.org/cgi/collection/oceans>